Chinese Journal of
POLYMER SCIENCE

RESEARCH ARTICLE

https://doi.org/10.1007/s10118-023-3033-0
Chinese J. Polym. Sci. **2024**, *42*, 364–372

Simultaneous Bulk- and Surface-initiated Living Polymerization Studied with a Heterogeneous Stochastic Reaction Model

Jia-Shu Ma[a], Zhi-Ning Huang[a], Jia-Hao Li[a], Bang-Ping Jiang[a], Yan-Da Liao[b], Shi-Chen Ji[a*], and Xing-Can Shen[a*]

[a] *State Key Laboratory for Chemistry and Molecular Engineering of Medicinal Resources, Key Laboratory for Chemistry and Molecular Engineering of Medicinal Resources (Ministry of Education of China), School of Chemistry and Pharmaceutical Sciences, Guangxi Normal University, Guilin 541004, China*
[b] *School of Computer Science and Engineering & School of Software, Guangxi Normal University, Guilin 541004, China*

Electronic Supplementary Information

Abstract To better characterize the properties of surface-initiated polymers, simultaneous bulk- and surface-initiated polymerizations are usually carried out by assuming that the properties of the surface-initiated polymers resemble those of the bulk-initiated polymers. Through a Monte Carlo simulation using a heterogeneous stochastic reaction model, it was discovered that the bulk-initiated polymers exhibit a higher molecular weight and a lower dispersity than the corresponding surface-initiated polymers, which indicates that the equivalent assumption is invalid. Furthermore, the molecular weight distributions of the two types of polymers are also different, suggesting different polymerization mechanisms. The results can be simply explained by the heterogeneous distributions of reactants in the system. This study is helpful to better understand surface-initiated polymerization.

Keywords Surface-initiated polymerization; Polymer brush; Stochastic reaction model; Heterogeneous polymerization; Simultaneous polymerization

Citation: Ma, J. S.; Huang, Z. N.; Li, J. H.; Jiang, B. P.; Liao, Y. D.; Ji, S. C.; Shen, X. C. Simultaneous bulk- and surface-initiated living polymerization studied with a heterogeneous stochastic reaction model. *Chinese J. Polym. Sci.* **2024**, *42*, 364–372.

INTRODUCTION

Surface-initiated polymerization (SIP) is a powerful technique that involves immobilized initiators on substrate surfaces to grow polymer chains, resulting in systems with high grafting density and layer thickness, known as polymer brushes. Polymer brushes have found extensive applications in diverse fields, such as corrosion-protection coatings, adhesives, protein-resistant surfaces, chemical lubricants, and antifouling.[1–7] Consequently, understanding the underlying mechanism of SIP has become a subject of significant interest to better tailor the properties of polymer brushes and enhance material performance.

The properties of grafted polymers, such as molecular weight, molecular weight distribution, and dispersity, are key parameters for designing materials with specific properties. For example, a polymer brush with a low dispersity displays an improved anti-fouling performance.[8] However, it is challenging to characterize these properties of surface-initiated polymers with methods like GPC due to the small amount of the product obtained from SIPs, especially those on flat surfaces. Additionally, cleavage of polymer chains from the substrate is required for characterization, which might alter the properties of polymers.[9]

An alternative method, widely applied in research, involves conducting simultaneous bulk- and surface-initiated polymerization by adding extra free initiators to the SIP system (Fig. 1).[10–12] This approach assumes that the properties of the surface-initiated polymers resemble those of the bulk-initiated polymers. Then the properties of grafted polymers

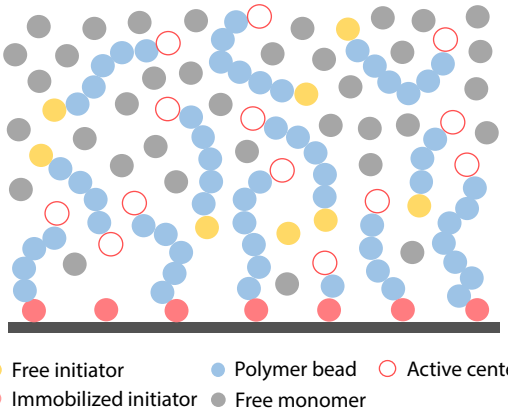

Fig. 1 Illustration of a simultaneous bulk- and surface-initiated living polymerization.

* Corresponding authors, E-mail: shichen.ji@mailbox.gxnu.edu.cn (S.C.J.)
E-mail: xcshen@mailbox.gxnu.edu.cn (X.C.S.)

Invited Research Article of Special Issue on "Theory and Simulation of Macromolecules"
Received July 19, 2023; Accepted August 5, 2023; Published online September 15, 2023

can be estimated by characterizing free polymers. However, the validity of the equivalent assumption is still in debate. Contradictory results have been reported in different experiments, as reviewed by Zoppe *et al*.[9]

To overcome the limitations of experiments and theoretical approaches, computer simulations have emerged as a powerful research tool.[13–16] Since the pioneering work by Genzer,[17] various simulations have been developed to study the mechanism of SIP.[17–33] These studies have revealed that SIP typically results in larger dispersity and smaller molecular weight compared to corresponding bulk-initiated polymerization, except when the grafting density is very low. Studies have also examined the simultaneous bulk- and surface-initiated polymerization to validate the equivalent assumption adopted in experiments.[22–25,32] The results demonstrate that the equivalent assumption is generally invalid, since the bulk-initiated polymers usually show a larger molecular weight and a lower dispersity than those of surface-initiated polymers.

However, in many simulations, all active centers react with equal probability, implying a homogeneous reaction system.[17–19,27–33] It neglects the fact that SIP is a heterogeneous polymerization. As polymerization progresses, the nascent polymer chains formed at the surface will expel free monomers from the surface, which leads to a heterogeneous distribution of monomers and active ends. We can anticipate that polymers with active ends located further from the surface should react with larger probabilities due to the higher local concentration of free monomers.

Recently, we proposed a stochastic reaction model (SRM) for heterogeneous polymerizations.[34,35] In this model, the reaction probability between an active end and a nearby free monomer is determined based on the local concentration of free monomers. As a result, each active end reacts with its own probability, and the heterogeneous reaction environment is well considered. By applying both the heterogeneous and traditional SRMs, we confirmed that the heterogeneous reaction environment plays an important role in SIP, which significantly affects the properties like dispersity and molecular weight distribution.[34]

Our finding suggests that it is necessary to reexamine simultaneous bulk- and surface-initiated polymerization. In this paper, we applied the heterogenous SRM to investigate simultaneous polymerization. The results not only confirmed the invalidity of the equivalent assumption adopted in experiments, but also provided valuable information on properties like molecular weight distribution. This study sheds light on a better understanding of the underlying mechanism of SIP.

MODELS AND SIMULATION METHODS

The simulation was carried out in a simple cubic lattice with a volume $V = L_x \times L_y \times L_z$ with periodic boundary conditions in both x and z directions. There were two impenetrable walls at y=1 and L_y respectively. The Larson-type bond fluctuation model was adopted, which has been described in our previous studies.[34–37] Briefly, each monomer or initiator occupies only one lattice site, and the bond length is 1 or $\sqrt{2}$. During relaxation, a monomer/initiator is randomly selected and attempted to move to one of its 18 nearest and next nearest neighbour sites, with permitted bond lengths and no bond crossings occurring. The unit simulation time, MC step (MCs), is defined as all monomers and initiators are tried to move once on average.

The polymerization was carried out after relaxing every τ MCs. By adjusting the reaction interval time τ, the system can be tuned as either diffusion- or reaction-controlled.[34,35] During the polymerization process, (i) an initiator or active center is selected at random; (ii) the number m of free monomers within the radius of $\sqrt{2}$ is then determined; (iii) the initiator or active center attempts to react with one of these m free monomers with probability mP_0, where P_0 is a constant representing the reaction probability between one active center and one free monomer. Since the reaction probability is determined by the local monomer concentration, this SRM is well-suited for studying heterogeneous polymerization systems like SIP.[34,35]

In this simulation, only chain propagation was considered, which corresponds to living polymerization. The monomer conversion C of a bulk-initiated living polymerization can be calculated as:[34,35]

$$C = 1 - \exp(-(m_{max} - 1)[I]_0 P_0 t/\tau) \quad (1)$$

where m_{max} is the maximum number of free monomers around an initiator/active center and equals 18 in this simulation; $[I]_0$ is the initial number of initiators. This equation can be used to verify the accuracy of the simulation results.

RESULTS AND DISCUSSION

Validation of the Equivalent Assumption

Firstly, we examined a simultaneous polymerization with a high grafting density σ=0.5. Other parameters are as follows. The size of the simulation box is L_x=40, L_z=36, and L_y=302. The initial monomer concentration is $[M]_0$=0.4 monomer per lattice. Strictly speaking, it is a solution polymerization rather than a bulk polymerization, but in the following, we do not make a strict distinction. Both the number of immobilized initiators on the surface I_S and that of free initiators in the bulk I_B equals 720, thus the fraction of immobilized initiators is f=0.5. The reaction interval time τ is 10, the reaction probability is P_0=0.001, and the simulation time is 2×10^6 MCs. In the beginning, all the monomers and initiators were randomly distributed in the system (immobilized initiators were randomly located on the y=1 surface). The system was relaxed for 10^3 MCs to eliminate the influence of the initial state and served as an input to the reactive simulations. The results were averaged for 20 independent runs.

According to the monomer conversion, simultaneous polymerization is slower than the theoretical predication of bulk-initiated living polymerization (Fig. 2a). A greater proportion of reacted monomers has converted into free chains than grafted ones (Fig. 2a). Fig. 2(b) illustrates that free initiators have been consumed within 10^4 MCs. The number of unreacted free initiators exponentially decays according to:[18]

$$I = I_0(1 - P_r)^{t/\tau} \quad (2)$$

where P_r is the reaction probability and is calculated as $(m_{max} - 1)[M]_0 P_0$ (the inlet of Fig. 2b). Meanwhile the immobilized initiators on the surface reacted slowly, with a 92%

conversion achieved at t=3×10^4 MCs.

Both the number average molecular weights of free chains $M_{n,f}$ and grafted chains $M_{n,g}$ increase linearly with monomer conversion, but $M_{n,f}$ increases more quickly than $M_{n,g}$ (Fig. 2c). At the end of the reaction, $M_{n,f}$ is as high as 167, more than twice of $M_{n,g}$=73. In addition to molecular weight, there is also a significant difference in the dispersity ($Đ$) between free and grafted polymers, with grafted chains having a much larger $Đ$ compared to free ones (Fig. 2d). Since the properties of free chains are quite different from those of grafted chains in simultaneous polymerization, the equivalent assumption cannot be applied to estimate the properties of grafted chains, consistent with previous simulations.[22–25]

The advantage of the heterogeneous SRM is that it can provide accurate information on molecular weight distribution (MWD). In simultaneous polymerization, the MWDs of free and grafted polymers are different in both the locations and shapes (Fig. 3). At low monomer conversion C, the MWD of free polymers is symmetry and can be described by the Poisson distribution

$$P(N) = \frac{M_n^N}{N!}\exp(-M_n) \quad (3)$$

However, with increasing C, the shape gradually deviates from the Poisson distribution and more shorter chains can be observed (Fig. 3a). For the grafted polymers, the MWD is much broader compared to that of free polymers, which seems to be a bimodal distribution at high monomer conversion (Fig. 3b).

Spatial Distributions in the System

As known, reaction kinetics is determined by both the concentrations and spatial distributions of reactants. To gain further insights into simultaneous polymerization, we analyzed the density profiles of various species at different distances to the surface. Fig. 4 shows the results at monomer conversion C=0.6. Free monomers display a nearly constant density ρ_M = 0.19 at large distances from the surface (Fig. 4a). However, near the surface, a very low ρ_M = 0.03 is observed. Such a large divergence in ρ_M suggests the breakdown of the equivalent assumption, as the reaction environments of grafted and free polymers are different. Grafted polymers, with active ends located near the surface, react in a region with a low and gradually varying concentration of free monomers. On the contrary, most free polymers react in a similar environment with a higher concentration of free monomers. Consequently, a smaller molecular weight and a large dispersity are expected for grafted polymers. Fig. 4(a) also suggests that some free

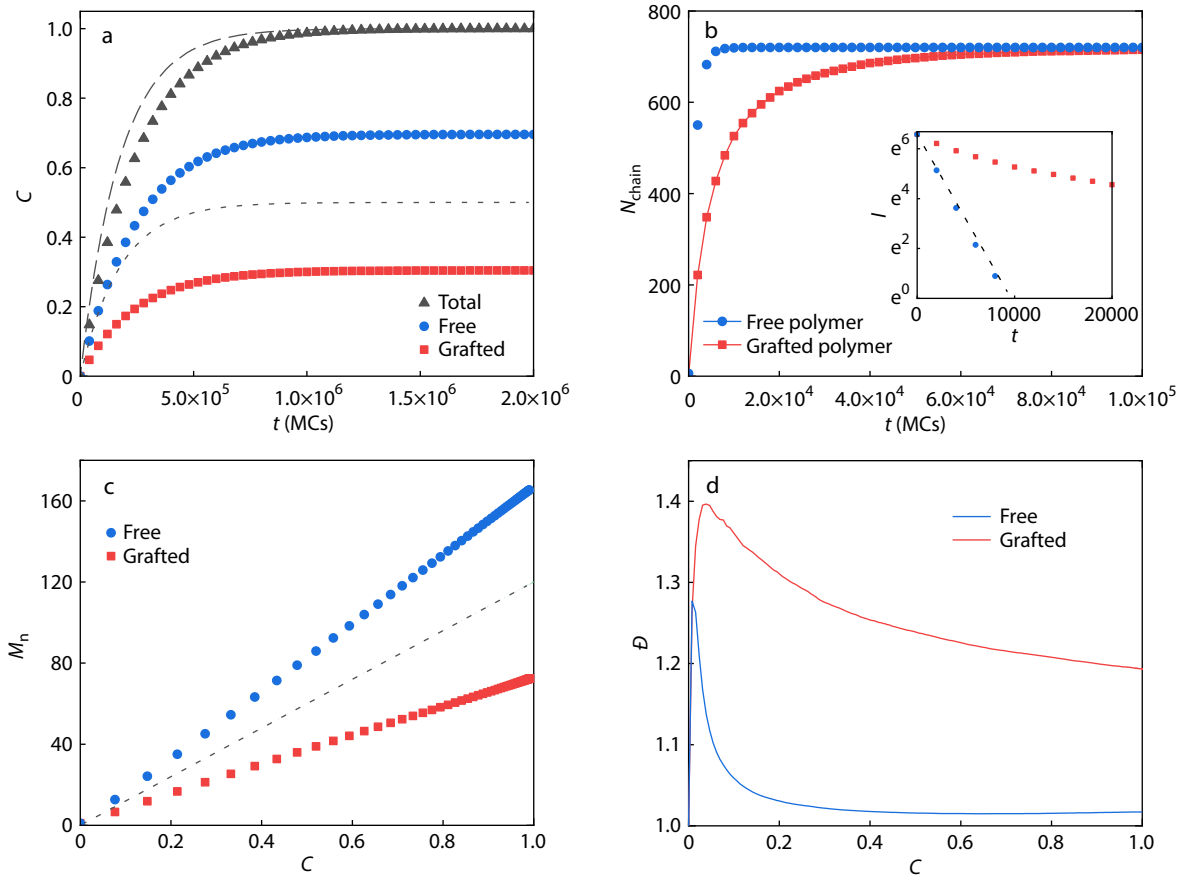

Fig. 2 (a) Time evolution of monomer conversion and the proportions of monomers that formed free and grafted chains respectively. The dashed line is the theoretical prediction. The dotted line is half the value of the dashed line. (b) The number of free and grafted chains. The inlet shows the number of unreacted free and immobilized initiators. The number average molecular weight (c) and dispersity (d) of free and grafted polymers as a function of monomer conversion. Error bar is not given as it is shorter than the size of the symbol as seen from Fig. S1 in the electronic supplementary information, ESI).

https://doi.org/10.1007/s10118-023-3033-0

polymers react in a region with low monomer concentration (y<90), so the corresponding molecular weight distribution of free polymers deviates from the Poisson distribution which is typically observed in ideal living polymerizations.

Since the density of polymers and that of monomers are closely related, analysing the density of polymers can explain the origin of the heterogeneous distribution of free monomers. Grafted polymers exhibit a high density $\rho_{P,g}$=0.83 near the surface, which linearly decreases with increasing distance y from the surface (Fig. 4a). At the periphery of the brush, $\rho_{P,g}$ rapidly decreases and eventually vanishes at y=50. Meanwhile, free polymers show a nearly constant density $\rho_{P,f}$=0.17 for distances y>90. Interestingly, a peak is observed before $\rho_{P,f}$ reaches zero. Since $\rho_{P,g}$ is much larger than $\rho_{P,f}$, there are fewer free monomers near the surface due to the excluded volume effect of polymers, resulting in the heterogeneous distribution of monomers.

We would like to further discuss the difference between this system and the one with a polymer brush immersed in a polymer solution. The latter system usually consists of monodispersed polymer chains and equilibrium properties are concerned.[38,39] The brush is compressed and shows a parabolic density profile. Free polymers partially penetrate the brush, and the density smoothly diminishes to zero. While in this study, the density of polymer brush shows a linear decrease, caused by the large dispersity.[34,40] Notably, the peak

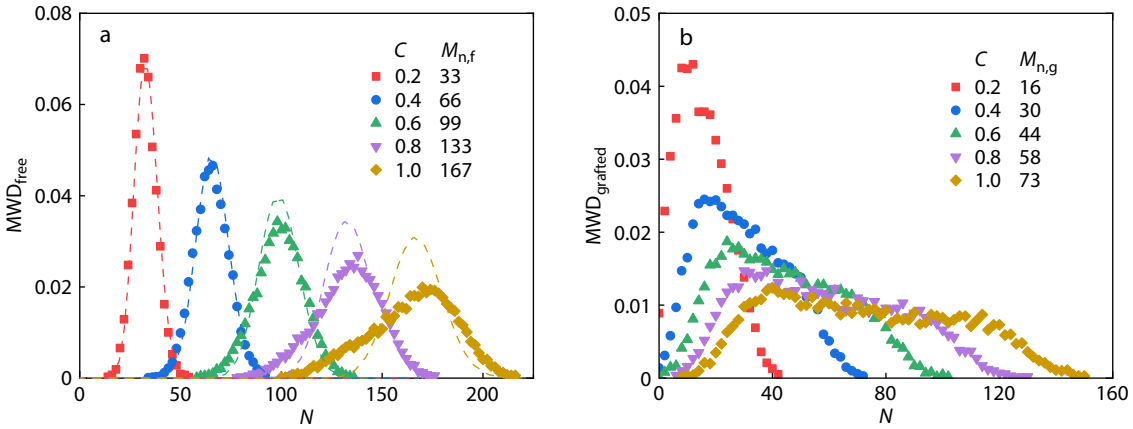

Fig. 3 The molecular weight distributions of free (a) and grafted (b) polymers at given monomer conversions. The dotted lines are the corresponding theoretical results of Poisson distributions.

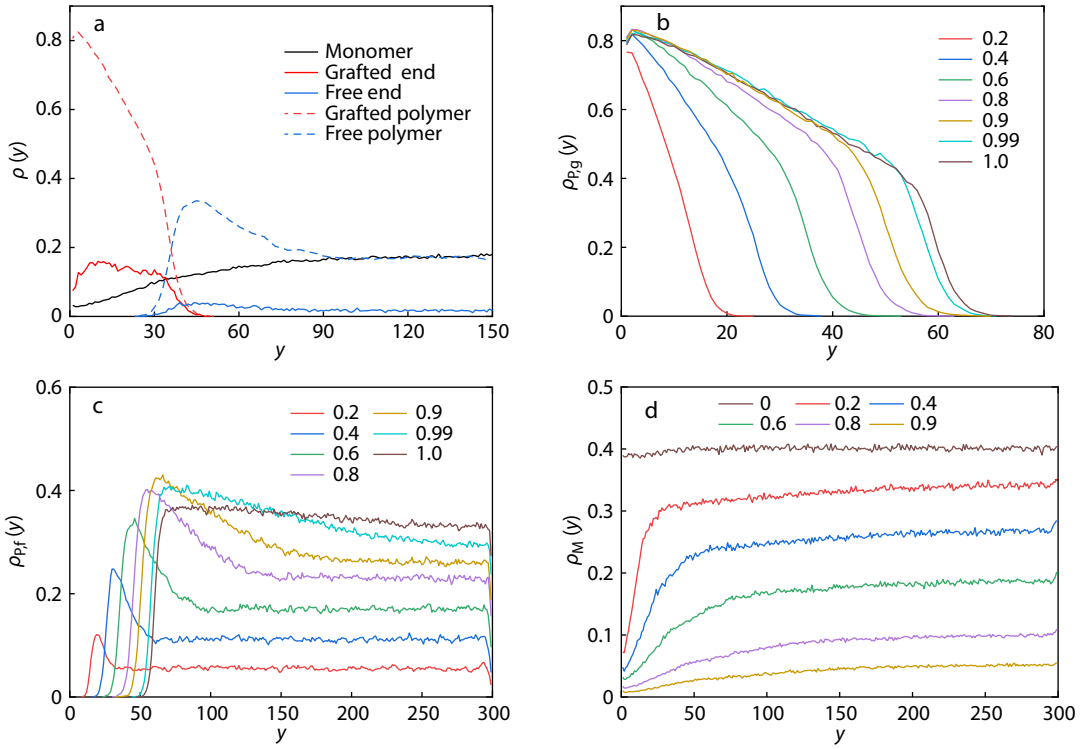

Fig. 4 (a) Density profiles of different species at monomer conversion C=0.6. The densities of active ends have been enlarged ten times for a better view. Density profiles of grafted polymers (b), free polymers (c), and free monomers (d) with given monomer conversions.

https://doi.org/10.1007/s10118-023-3033-0

observed in the density of free polymers reflects the dynamic nature of the polymerization. As polymerization processes, grafted polymers formed near the surface (Fig. 4b) push free polymers away from the surface (Fig. 4c), creating a dense region of free polymers. This peak eventually disappears at the end of the polymerization. Meanwhile, free monomers evolve from a homogenous distribution to a heterogenous distribution (Fig. 4d). The density profiles of other species during polymerization are shown in Fig. S2 (in ESI).

Effect of Grafting Density

To investigate the effect of grafting density σ, we varied the height and lateral size of the simulation box while keeping the number of immobilized initiators, monomer concentration, total volume, and other parameters constant. At low grafting densities, both the molecular weights of free and grafted polymers are close to the theoretical predictions (Fig. 5a). As grafting density increases, a divergence in molecular weight emerges. At the same monomer conversion, the molecular weight of free polymers increases with σ, while that of grafted polymers decreases. The relationship between the molecular weight of free and grafted chains is shown in Fig. 5(b), which obviously increases with σ. For example, at σ=0.6, the molecular weight of free polymers can be 2.8 times greater than that of grafted polymers (Fig. 5b). Additionally, the influence of grafting density on dispersity differs between the two polymers. The dispersity of free polymers is negligibly influenced by σ (Fig. 5c), meanwhile, that of grafted polymers significantly increases with σ (Fig. 5d).

We compared the MWDs of different systems with a monomer conversion C=0.5. When grafting density is low (σ=0.1), the MWD of free polymers follows a Poisson distribution (Fig. 6a), while a slight deviation is observed in the MWD of grafted polymers (Fig. 6b). As the grafting density increases, the MWDs of free/grafted polymers gradually shift to the right/left direction, corresponding to their molecular weight change as shown in Fig. 5(a). Notably, the differences in the shape of the MWDs between the two types of polymers become increasingly evident with increasing grafting density. As aforementioned, it can be simply explained by the reactant distributions in space. The maximum density of grafted polymers increases with grafting density (Fig. 6c), thus the distribution of free monomers becomes more heterogenous (Fig. 6d).

Effect of the Fraction of Immobilized Initiators

We further examined the fraction of immobilized initiators f by fixing the number of immobilized initiators and varying the number of free initiators. The height of the simulation box is adjusted to keep the designed chain length constant. Both the molecular weights of free and grafted polymers increase with the fraction of immobilized initiators at grafting density 0.2 and 0.5, respectively (Figs. 7a and 7c). However, the relative molecular weight between free and grafted polymers seems insensitive to the fraction of immobilized initiators (Figs. 7b and 7d). At low molecular weight, all data fall onto the same line. At

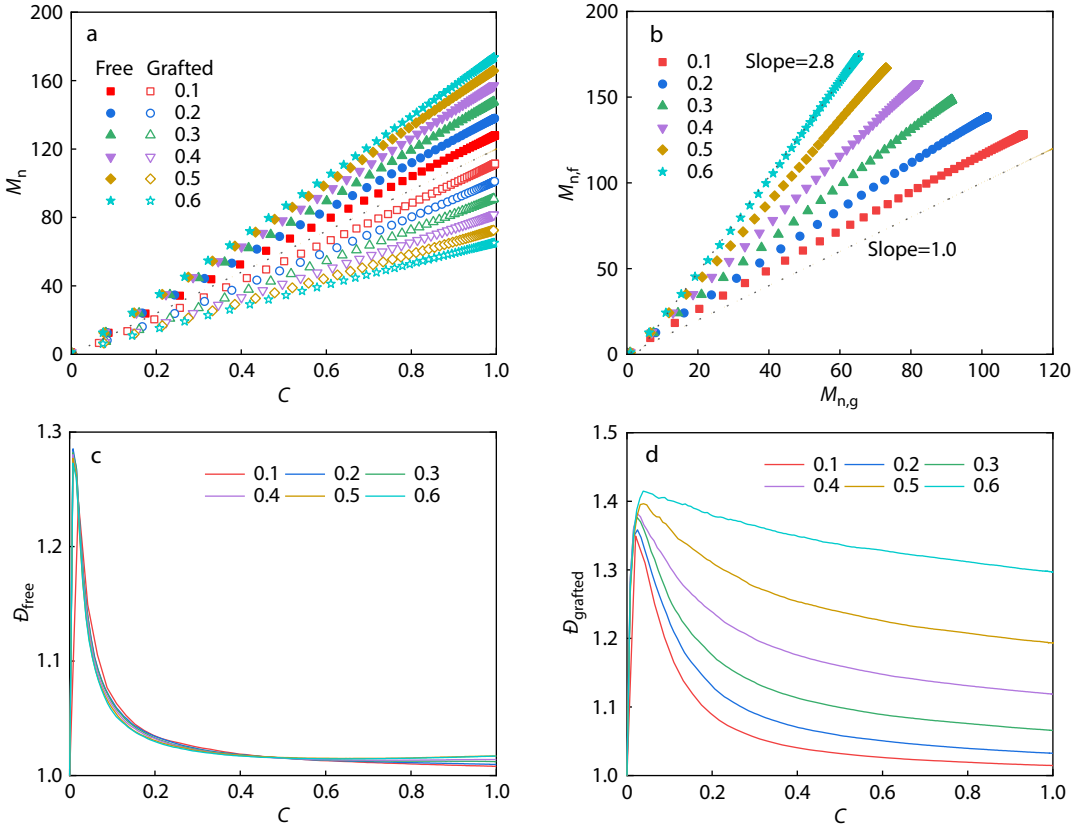

Fig. 5 Effect of grafting density. (a) The molecular weight of free and grafted polymers during polymerization; (b) The number average molecular weight of free polymers versus that of grafted polymers; The dispersity of free (c) and grafted (d) polymers during polymerization.

https://doi.org/10.1007/s10118-023-3033-0

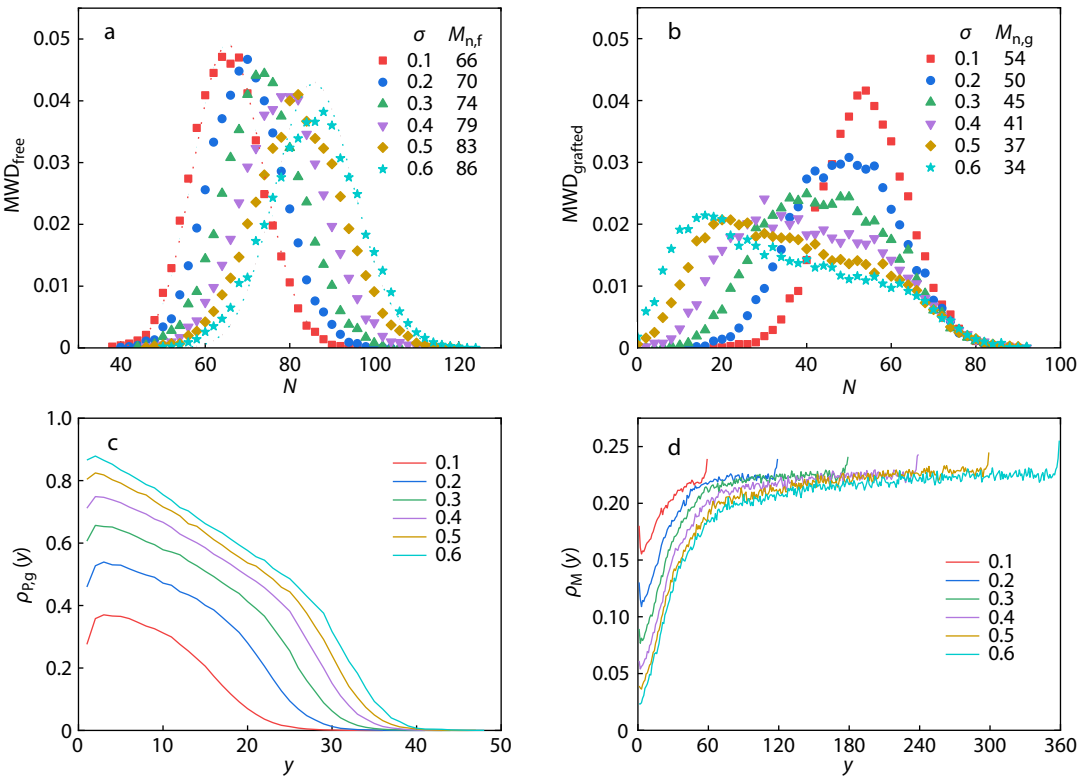

Fig. 6 Effect of grafting density. Molecular weight distributions of free (a) and grafted (b) polymers at monomer conversion C=0.5 with indicated number average molecular weight. The dotted lines are calculated according to the Poisson distribution. The density profiles of grafted polymers (c) and free monomers (d).

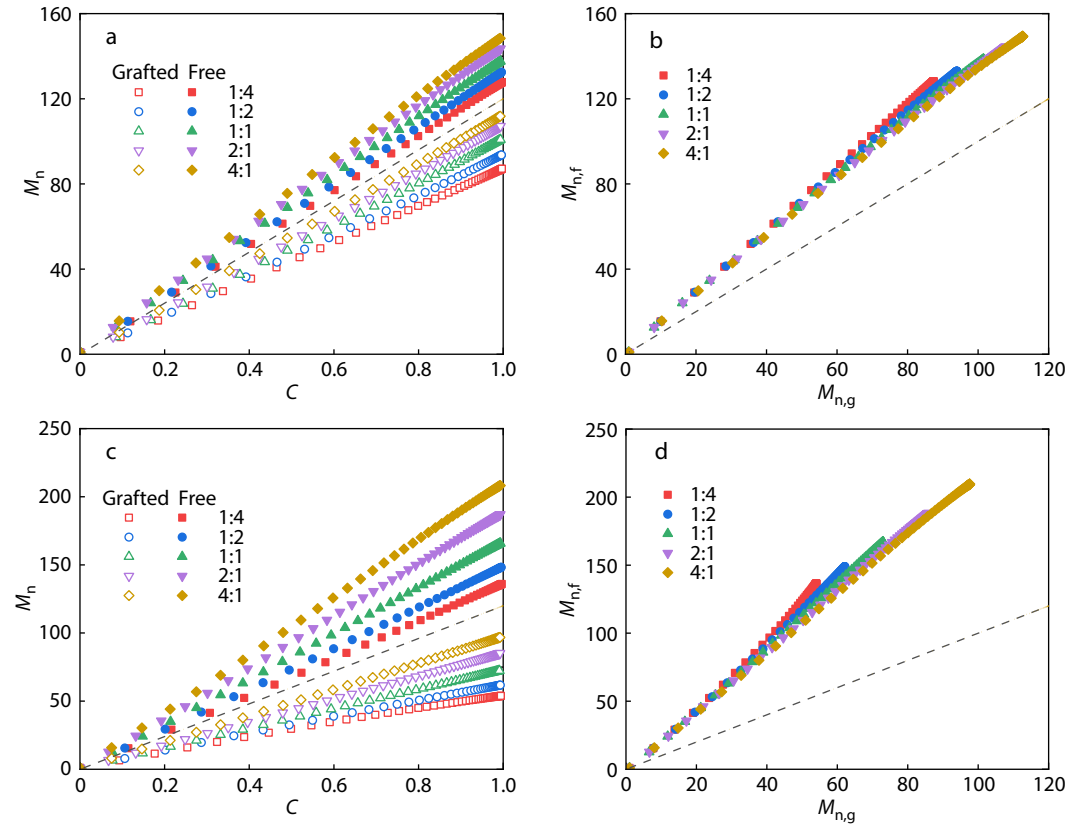

Fig. 7 The molecular weight of free and grafted polymers during polymerization at grafting density of (a) 0.2 and (c) 0.5 with given ratios between the immobilized and free initiators. The relative molecular weights between free and grafted polymers versus that of grafted polymers at grafting density of (b) 0.2 and (d) 0.5.

https://doi.org/10.1007/s10118-023-3033-0

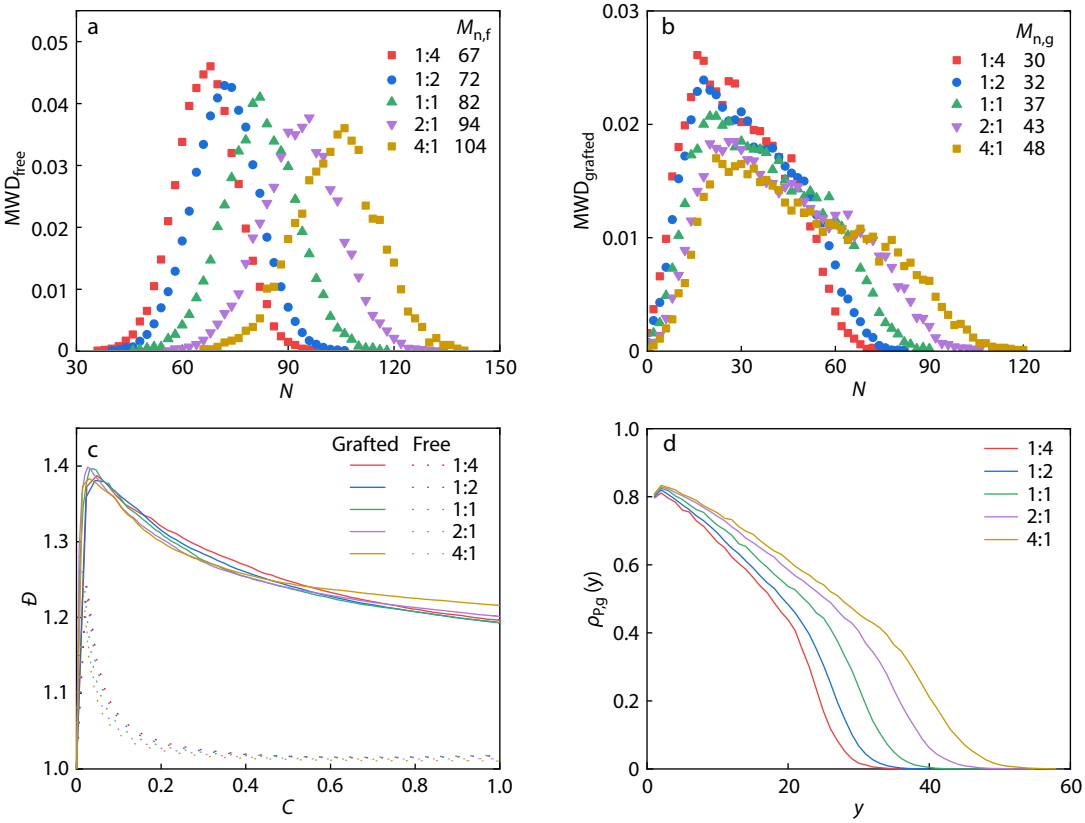

Fig. 8 Molecular weight distributions of (a) free and (b) grafted polymers. The grafting density is 0.5, monomer conversion is 0.5. The number average molecular weights of free and grafted polymers are shown. (c) Dispersity of free and grafted polymers during polymerization. (d) The density profiles of grafted polymers.

high molecular weight, the relative molecular weight slightly declines with increasing *f*.

The molecular weight distributions are compared at the same monomer conversion *C*=0.5. Similar trends are found for grafting density σ=0.5 (Fig. 8) and σ=0.2 (Fig. S3 in ESI). For both free and grafted polymers, the positions of MWDs shift towards higher molecular weight with an increasing fraction of immobilized initiators *f* (Figs. 8a and 8b). However, the dispersity seems insensitive to *f* (Fig. 8c). This observation can be explained by the fact that the maximum value of the brush density is mainly affected by the grafting density instead of the molecular weight, as shown in Fig. 8(d).[41,42] This finding differs from the results obtained by Turgman-Cohen and Genzer, which may be attributed to the use of different stochastic reaction models.[23,24] In the literature, all active ends react with the same probability by assuming that the system is well mixed, which is a SRM for homogenous polymerization systems.[23,24] Consequently, the heterogeneous reaction environment in SIP was neglected in those studies, whereas it was adequately considered in our investigation.

CONCLUSIONS

In this study, we employed Monte Carlo simulations to investigate simultaneous bulk- and surface-initiated living polymerization using a heterogeneous stochastic reaction model. The widely adopted equivalent assumption that the properties of surface-initiated polymers resemble those of bulk-initiated polymers was found to be invalid based on our simulation results. Surface-initiated polymers usually show a smaller molecular weight, lower dispersity, and broader molecular weight distribution compared to free-initiated polymers.

The distinct properties of bulk- and surface-initiated polymers can be explained by the heterogeneous distribution of reactants in the system, which is a characteristic of SIP. Due to the exclusion of nascent polymer brush, there are fewer free monomers near the surface, leading to different reaction environments for bulk- and surface-initiated polymerizations and resulting in divergent polymerization behavior.

The heterogeneous spatial distributions of reactants are closely related to the density profile of the polymer brush. Factors influencing the density profile of the polymer brush can impact the polymerization process. In this study, we primarily focused on the effects of grafting density and the ratio of immobilized initiators. However, other factors such as polymerization rate, surface curvature, and solvent quality may also play a role in the polymerization process. Among these factors, grafting density emerges as the most significant one, significantly affecting the maximum density profile of the polymer brush and the system's heterogeneity.

In conclusion, this study confirms the invalidity of the equivalent assumption and highlights the crucial role of the heterogeneous reaction environment in surface-initiated poly-

https://doi.org/10.1007/s10118-023-3033-0

merization. The spatial distributions of reactants (free monomers and active ends) and products (polymer brush) are closely interconnected and mutually influenced. Utilizing existing knowledge of polymer brushes can help to better understand the underlying mechanism of SIP. Furthermore, numerical analysis of SIP is called for a qualitative description such as monomer conversion and molecular weight distribution in future studies.

Conflict of Interests

The authors declare no interest conflict.

Electronic Supplementary Information

Electronic supplementary information (ESI) is available free of charge in the online version of this article at http://doi.org/10.1007/s10118-023-3033-0.

ACKNOWLEDGMENTS

This work was financially supported by the National Natural Science Foundation of China (No. 22263002) and the "Overseas 100 Talents Program" of Guangxi Higher Education.

REFERENCES

1 Chen, W. L.; Cordero, R.; Tran, H.; Ober, C. K. 50th Anniversary perspective: polymer brushes: novel surfaces for future materials. *Macromolecules* **2017,** *50*, 4089−4113.
2 Murad Bhayo, A.; Yang, Y.; He, X. Polymer brushes: synthesis, characterization, properties and applications. *Prog. Mater Sci.* **2022**, *130*, 101000.
3 Feng, C.; Huang, X. Polymer brushes: efficient synthesis and applications. *Acc. Chem. Res.* **2018**, *51*, 2314−2323.
4 Pester, C. W.; Benetti, E. M. Modulation of polymer brush properties by tuning dispersity. *Adv. Mater. Interfaces* **2022**, *9*, 2201439.
5 Wang, R.; Wei, Q.; Sheng, W.; Yu, B.; Zhou, F.; Li, B. Driving polymer brushes from synthesis to functioning. *Angew. Chem. Int. Ed.* **2023**, *62*, e202219312.
6 Zhang, R.; Liu, Y.; He, M.; Su, Y.; Zhao, X.; Elimelech, M.; Jiang, Z. Antifouling membranes for sustainable water purification: strategies and mechanisms. *Chem. Soc. Rev.* **2016**, *45*, 5888−5924.
7 Chen, Q.; Yu, S.; Zhang, D.; Zhang, W.; Zhang, H.; Zou, J.; Mao, Z.; Yuan, Y.; Gao, C.; Liu, R. Impact of antifouling PEG layer on the performance of functional peptides in regulating cell behaviors. *J. Am. Chem. Soc.* **2019**, *141*, 16772−16780.
8 Zhang, P.; Zhang, Z.; Wang, D.; Hao, J.; Cui, J. Monodispersity of poly(ethylene glycol) matters for low-fouling coatings. *ACS Macro Lett.* **2020**, *9*, 1478−1482.
9 Zoppe, J. O.; Ataman, N. C.; Mocny, P.; Wang, J.; Moraes, J.; Klok, H. A. Surface-initiated controlled radical polymerization: state-of-the-art, opportunities, and challenges in surface and interface engineering with polymer brushes. *Chem. Rev.* **2017**, *117*, 1105−1318.
10 Husseman, M.; Malmström, E. E.; McNamara, M.; Mate, M.; Mecerreyes, D.; Benoit, D. G.; Hedrick, J. L.; Mansky, P.; Huang, E.; Russell, T. P. Controlled synthesis of polymer brushes by "living" free radical polymerization techniques. *Macromolecules* **1999**, *32*, 1424−1431.
11 Tsujii, Y.; Ejaz, M.; Sato, K.; Goto, A.; Fukuda, T. Mechanism and kinetics of RAFT-mediated graft polymerization of styrene on a solid surface. 1. Experimental evidence of surface radical migration. *Macromolecules* **2001**, *34*, 8872−8878.
12 Kruk, M.; Dufour, B.; Celer, E. B.; Kowalewski, T.; Jaroniec, M.; Matyjaszewski, K. Grafting monodisperse polymer chains from concave surfaces of ordered mesoporous silicas. *Macromolecules* **2008**, *41*, 8584−8591.
13 Binder, K.; Milchev, A. Polymer brushes on flat and curved surfaces: how computer simulations can help to test theories and to interpret experiments. *J. Polym. Sci., Part B: Polym. Phys.* **2012**, *50*, 1515−1555.
14 Xu, D.; Wan, H. X.; Yao, X. R.; Li, J.; Yan, L. T. Molecular simulations in macromolecular science. *Chinese J. Polym. Sci.* **2023**, *41*, 1361−1370.
15 Liang, C. X.; Lu, H.; Huang, B. Y.; Xing, J. Y.; Gu, F. L.; Liu, H. Physical insight for grafting polymer chains onto the substrate *via* computer simulations: kinetics and property. *Chinese J. Polym. Sci.* **2022**, *40*, 817−833.
16 Hu, W. B. Computer simulation of polymers: bridging the gap between theory and experiment. *Chinese J. Polym. Sci.* **2022**, *40*, 709−710.
17 Genzer, J. In silico polymerization: computer simulation of controlled radical polymerization in bulk and on flat surfaces. *Macromolecules* **2006**, *39*, 7157−7169.
18 Liu, H.; Li, M.; Lu, Z. Y.; Zhang, Z. G.; Sun, C. C. Influence of surface-initiated polymerization rate and initiator density on the properties of polymer brushes. *Macromolecules* **2009**, *42*, 2863−2872.
19 Turgman-Cohen, S.; Genzer, J. Computer simulation of controlled radical polymerization: effect of chain confinement due to initiator grafting density and solvent quality in "grafting from" method. *Macromolecules* **2010**, *43*, 9567−9577.
20 Bain, E. D.; Turgman-Cohen, S.; Genzer, J. Progress in computer simulation of bulk, confined, and surface-initiated polymerizations. *Macromol. Theory Simul.* **2013**, *22*, 8−30.
21 Deng, B.; Palermo, E. F.; Shi, Y. Comparison of chain-growth polymerization in solution versus on surface using reactive coarse-grained simulations. *Polymer* **2017**, *129*, 105−116.
22 Polanowski, P.; Hałagan, K.; Pietrasik, J.; Jeszka, J. K.; Matyjaszewski, K. Growth of polymer brushes by "grafting from" *via* ATRP-Monte Carlo simulations. *Polymer* **2017**, *130*, 267−279.
23 Turgman-Cohen, S.; Genzer, J. Simultaneous bulk- and surface-initiated controlled radical polymerization from planar substrates. *J. Am. Chem. Soc.* **2011**, *133*, 17567−17569.
24 Turgman-Cohen, S.; Genzer, J. Computer simulation of concurrent bulk-and surface-initiated living polymerization. *Macromolecules* **2012**, *45*, 2128−2137.
25 Arraez, F. J.; Van Steenberge, P. H.; D'hooge, D. R. Conformational distributions near and on the substrate during surface-initiated living polymerization: a lattice-based kinetic Monte Carlo approach. *Macromolecules* **2020,** 4630−4648.
26 Arraez, F. J.; Van Steenberge, P. H.; D'hooge, D. R. The competition of termination and shielding to evaluate the success of surface-initiated reversible deactivation radical polymerization. *Polymers* **2020**, *12*, 1409.
27 Yan, Y. D.; Xue, Y. H.; Zhao, H. Y.; Liu, H.; Lu, Z. Y.; Gu, F. L. Insight into the polymerization-induced self-assembly *via* a realistic computer simulation strategy. *Macromolecules* **2019**, *52*, 6169−6180.
28 Liu, H.; Zhu, Y. L.; Lu, Z. Y.; Müller-Plathe, F. A kinetic chain growth algorithm in coarse-grained simulations. *J. Comput. Chem.* **2016**, *37*, 2634−2646.
29 Berezkin, A. V.; Kudryavtsev, Y. V. Simulation of end-coupling

reactions at a polymer-polymer interface: the mechanism of interfacial roughness development. *Macromolecules* **2011**, *44*, 112−121.
30 Akkermans, R. L. C.; Toxvaerd, S. R.; Briels, W. J. Molecular dynamics of polymer growth. *J. Chem. Phys.* **1998**, *109*, 2929−2940.
31 de Buyl, P.; Nies, E. A parallel algorithm for step- and chain-growth polymerization in molecular dynamics. *J. Chem. Phys.* **2015**, *142*, 134102.
32 Xu, J.; Xue, Y. H.; Cui, F. C.; Liu, H.; Lu, Z. Y. Simultaneous polymer chain growth with the coexistence of bulk and surface initiators: insight from computer simulations. *Phys. Chem. Chem. Phys.* **2018**, *20*, 22576−22584.
33 Lu, W.; Ding, J. Dynamic Monte Carlo simulation of polymerization of amphiphilic macromers in a selective solvent and associated chemical gelation. *Macromolecules* **2006**, *39*, 7433−7440.
34 Yang, B.; Liu, S.; Ma, J.; Yang, Y.; Li, J.; Jiang, B. P.; Ji, S.; Shen, X. C. A Monte Carlo simulation of surface-initiated polymerization: heterogeneous reaction environment. *Macromolecules* **2022**, *55*, 1970−1980.
35 Ma, J.; Li, J.; Yang, B.; Liu, S.; Jiang, B. P.; Ji, S.; Shen, X. C. A simple stochastic reaction model for heterogeneous polymerizations. *Polymers* **2022**, *14*, 3269.
36 Ji, S.; Ding, J. Rheology of polymer brush under oscillatory shear flow studied by nonequilibrium Monte Carlo simulation. *J. Chem. Phys.* **2005**, *123*, 144904.
37 Zhang, J. Z.; Peng, X. Y.; Liu, S.; Jiang, B. P.; Ji, S.; Shen, X. C. The persistence length of semiflexible polymers in lattice Monte Carlo simulations. *Polymers* **2019**, *11*, 295.
38 Martin, J.; Wang, Z. G. Polymer brushes: scaling, compression forces, interbrush penetration, and solvent size effects. *J. Phys. Chem.* **1995**, *99*, 2833−2844.
39 Wijmans, C.; Zhulina, E.; Fleer, G. Effect of free polymer on the structure of a polymer brush and interaction between two polymer brushes. *Macromolecules* **1994**, *27*, 3238−3248.
40 Qi, S.; Klushin, L. I.; Skvortsov, A. M.; Schmid, F. Polydisperse polymer brushes: internal structure, critical behavior, and interaction with flow. *Macromolecules* **2016**, *49*, 9665−9683.
41 Milner, S. T.; Witten, T. A.; Cates, M. E. Effects of polydispersity in the end-grafted polymer brush. *Macromolecules* **1989**, *22*, 853−861.
42 Murat, M.; Grest, G. S. Structure of a grafted polymer brush: a molecular dynamics simulation. *Macromolecules* **1989**, *22*, 4054−4059.

https://doi.org/10.1007/s10118-023-3033-0